J. Fluid Mech. (1992), *vol.* 245, *pp.* 263–278

Convection onset for a binary mixture in a porous medium and in a narrow cell: a comparison

By WOLFGANG SCHÖPF

Physikalisches Institut der Universität Bayreuth, W-8580 Bayreuth, Germany

(Received 22 October 1991 and in revised form 19 March 1992)

The hydrodynamic equations describing the fluid motion in a narrow cell and in a porous medium become identical in the limit of infinite height-to-width ratio (Hele-Shaw limit) in the first and zero permeability in the second case. The properties of the convection onset are, however, indistinguishable from an experimental point of view away from these limits. For realistic (rigid, impermeable) boundary conditions the critical Rayleigh number, the critical wavenumber and in the case of a Hopf bifurcation additionally the critical frequency are derived in both cases for a binary fluid mixture. For the porous medium the assumption of zero permeability is usually a very good approximation. The critical values for the porous medium are compared to those of the narrow cell for different height-to-width ratios and the connection with experiments is discussed.

1. Introduction

Hydrodynamic instabilities like Rayleigh–Bénard convection play an important role in the investigation of pattern formation in non-equilibrium systems and in various bifurcation problems. Convection in a horizontal layer of a binary fluid heated from below has attracted considerable interest during the last few years. A binary fluid is a mixture of two (miscible) fluids, e.g. water–alcohol or ^{3}He–^{4}He. Owing to the two-component nature of the fluid, the Soret effect leads to an additional control parameter besides the Rayleigh number R, namely the separation ratio Ψ, which measures the stabilizing ($\Psi < 0$), or destabilizing ($\Psi > 0$) effect of concentration gradients. Depending on Ψ, above a critical temperature difference, convection may set in as a stationary roll pattern or via a Hopf bifurcation leading to travelling waves (for an overview see e.g. Gershuni & Zhukhovitskii 1976 or Platten & Legros 1983). Early studies by Nield (1967), Hurle & Jakeman (1971), Legros *et al.* (1975), Chock & Li (1975) and others were followed by more specialized work during the last few years. The bifurcation structure, the onset values and the nature of the various convective patterns have been investigated in great detail with high experimental precision (Lee, Lucas & Tyler 1983; Walden *et al.* 1985; Rehberg & Ahlers 1985; Moses & Steinberg 1986; Sullivan & Ahlers 1988; Lhost & Platten 1988, 1989; Bensimon *et al.* 1990; Kolodner, Glazier & Williams 1990; Schöpf & Rehberg 1992) and theoretically (Brand & Steinberg 1983; Knobloch 1986; Linz & Lücke 1987; Knobloch & Moore 1988; Cross & Kim 1988; Schöpf & Zimmermann 1989; Barten *et al.* 1989).

Of special interest are the features near the convection onset: the critical temperature difference ΔT_c, the critical wavenumber k_c and in the case of a Hopf bifurcation the critical frequency ω_c. These values have been calculated for binary

fluid mixtures in a laterally infinitely extended horizontal layer (in this paper referred to as 'bulk binary mixtures') with realistic (rigid and impermeable) boundary conditions first by Legros *et al.* (1975) and Chock & Li (1975). Later they were discussed in more detail by Knobloch & Moore (1988) and Cross & Kim (1988). For porous media, which are very important for various applications (e.g. geophysical problems) (Dullien 1979), much was done many years ago for the case of a simple fluid (Lapwood 1948; Elder 1967; Westbrook 1969; Kvernvold & Tyvand 1979). For binary mixtures only idealized boundary conditions have been used up to now, where the results can be given analytically (Brand & Steinberg 1983; Knobloch 1986). Although ones does not expect large changes for realistic boundary conditions, there are some qualitative differences near the codimension-2 point and in the wavenumber behaviour for positive Ψ. (This is analogous to bulk binary mixtures as discussed by Knobloch & Moore (1988) and Cross & Kim (1988).) Furthermore it is important for the experimentalist to know the correct critical numbers. One purpose of this paper is to calculate these values for a laterally infinitely extended porous medium with rigid, impermeable boundaries at top and bottom.

Another problem of great interest is the convection onset in a narrow channel ('Hele-Shaw cell'), which has also been investigated for simple fluids (Hartline & Lister 1977; Frick & Clever 1980). With the term 'narrow channel' or 'narrow cell' a box with height d and width b is meant, where the height-to-width ratio $\gamma = d/b$ is of order one or larger. Such apparatuses, both of longitudinal and annular shape, are often used in experiments (Bensimon *et al.* 1990; Kolodner *et al.* 1990; Schöpf & Rehberg 1992), because they allow the investigation of two-dimensional roll patterns (with the roll axes parallel to the narrow dimension), which can be described very successfully by using one-dimensional Ginzburg–Landau equations (Bretherton & Spiegel 1983; Cross 1988; Thual & Fauve 1988; van Saarlos & Hohenberg 1990; Schöpf & Kramer 1991). This two-dimensional character persists up to high convection amplitudes and three-dimensional instabilities are avoided. For increasing γ it is no longer possible to compare the onset Rayleigh number to the one of bulk mixtures, because the friction due to the sidewalls becomes more and more important, leading to higher ΔT_c. The critical properties of a binary fluid mixture in such a convection channel of longitudinally infinite extent are calculated in this paper for realistic boundary conditions at top and bottom and rigid, impermeable, adiabatic sidewalls.

For both problems considered here it is useful to introduce new Rayleigh numbers R^{por} and R^{HS} which depend only linearly on the box height d (rather than $R^{\mathrm{b}} \propto d^3$ for bulk mixtures) and which contain a term describing the special properties. For the porous medium this is the permeability K and for the narrow cell an effective permeability K^{HS}, which characterizes the geometry (Hartline & Lister 1977; Brand & Steinberg 1983). For small K/d^2 and large γ (Hele-Shaw limit) the equations for both cases become identical. K is determined by the pore structure (Dullien 1979) and usually $0 < K/d^2 \ll 1$, so the first condition is fulfilled in most cases. It is interesting to know for which γ a porous medium can adequately be modelled by a narrow convection channel, because very often such boxes were used in laboratory experiments to simulate the fluid flow in a porous medium (see e.g. Elder 1967; Hartline & Lister 1977). This is due to the fact that the observation of flow phenomena within porous materials is difficult.

In §2 the basic equations for both the porous medium and the narrow cell together with the boundary conditions are presented. The equations for the deviations from the heat conduction state are given and the analogy between the two cases is

discussed. The different methods of solution for the linear stability analysis are outlined in §3. In §4 the results for the stationary and the oscillatory instabilities are given and compared for both geometries. The situation near the codimension-2 point is briefly discussed. Moreover, the results are compared with recent experiments. Section 5 is a short summary.

2. Basic equations and boundary conditions

2.1. *Porous medium*

2.1.1. *Pore structure*

To characterize a porous medium in physical terms various parameters can be introduced. The macroscopic parameters are determined by the pore structure of the medium, which is in general not known in detail. Two of these parameters, the *porosity* and the *permeability*, will enter the hydrodynamic equations (Dullien 1979).

The porosity ϵ (< 1, usually of order one) is defined as the ratio of the void space (that can be filled by fluid) and the bulk volume of the medium. The permeability K is a measure for the permeation of a Newtonian fluid through the porous medium and will in general be very small compared to d^2. Here d describes the macroscopic extension of the medium, in our case it is the height of the convection cell (see figure 1). Connections between ϵ and K can be formulated depending on the pore structure. If the medium consists of particles having more or less spherical shapes (see figure 1), the Kozeny formula can be used (Dullien 1979):

$$K = \frac{\epsilon^3 a^2}{150(1-\epsilon)^2}, \tag{2.1}$$

with a being the mean diameter of the particles. One necessary condition for a porous medium is $a \ll d$, therefore $K/d^2 \ll 1$ is always fulfilled. (The assumption of spherical particles is not a real restriction, because analogous formulae for other compositions of the medium lead to very small K/d^2, too (Dullien 1979).)

2.1.2. *Hydrodynamic equations*

The equations describing the fluid behaviour are influenced by the porous character of the medium and are slightly changed compared to those of bulk mixtures. More detailed statements concerning the controversial discussions about these equations are given by Dullien (1979) and Brand & Steinberg (1983). For the velocity $\boldsymbol{v}(\boldsymbol{r},t)$, the temperature $T(\boldsymbol{r},t)$, the concentration $N(\boldsymbol{r},t)$ and the pressure $p(\boldsymbol{r},t)$, we have in Boussinesq approximation (Gershuni & Zhukhovitskii 1976; Brand & Steinberg 1983):†

$$\boldsymbol{\nabla}\cdot\boldsymbol{v} = 0, \tag{2.2a}$$

$$\frac{\partial T}{\partial t} + (\boldsymbol{v}\cdot\boldsymbol{\nabla})\,T = \kappa\nabla^2 T, \tag{2.2b}$$

$$\frac{\partial N}{\partial t} + (\boldsymbol{v}\cdot\boldsymbol{\nabla})N = D\left(\nabla^2 N + \frac{k_T}{T_0}\nabla^2 T\right), \tag{2.2c}$$

$$\frac{1}{\epsilon}\frac{\partial \boldsymbol{v}}{\partial t} + a'\boldsymbol{v}F(|\boldsymbol{v}|) = -\frac{1}{\rho_0}\boldsymbol{\nabla}p - \frac{\nu}{K}\boldsymbol{v} + \frac{\rho}{\rho_0}\boldsymbol{g}. \tag{2.2d}$$

† Because the Dufour effect is negligible in fluid mixtures (Gershuni & Zhukhovitskii 1976; Platten & Legros 1983), the corresponding term is never included in this paper.

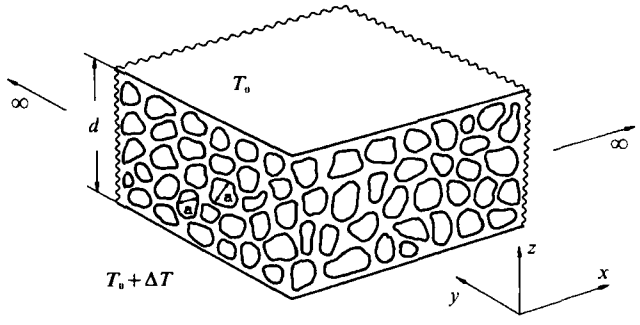

FIGURE 1. The model system for the porous medium consists of 'nearly' spherical particles with mean diameter a. They are placed between two horizontal boundaries with infinite extent in the (x, y)-direction. These plates are impermeable to mass flow and perfect heat conductors. The temperature at the top plate is T_0 and at the bottom plate $T_0+\Delta T$ with $\Delta T > 0$.

Equation (2.2a) is the continuity equation for an incompressible fluid. The heat equation (2.2b) is an average over both the porous medium and the fluid, because heat is transported by the fluid as well as by the medium. This leads to a mean thermal diffusivity $\kappa = [(1-\epsilon)\lambda_{\mathrm{sol}}+\epsilon\lambda_{\mathrm{liq}}]/(\rho_0 c_p)_{\mathrm{liq}}$ (here λ is the thermal conductivity and c_p the heat capacity, see Brand & Steinberg 1983). In equation (2.2c) for the concentration, D is the solutal diffusivity and k_T is the Soret coefficient, which measures the cross coupling between temperature gradients and mass fluxes and can have either plus or minus sign.

The Navier–Stokes equation (2.2d) contains the friction term $-(\nu/K)\,\boldsymbol{v}$, according to Darcy's law with the kinematic viscosity ν (Dullien 1979). The special form of the nonlinearity ($F(0) = 0$) will not be discussed here, because in what follows only linear properties are considered (for details, see Irmay 1958; Dullien 1979; Brand & Steinberg 1983; Knobloch 1986). The gravity field $\boldsymbol{g}$ is parallel to the z-direction: $\boldsymbol{g} = -g\boldsymbol{e}_z$. For the density ρ, a linearized state equation is used (Gershuni & Zhukhovitskii 1976):

$$\rho = \rho_0[1-\alpha(T-T_0)+\beta(N-N_0)], \tag{2.3}$$

with $\alpha = -(1/\rho_0)(\partial\rho/\partial T)$ and $\beta = (1/\rho_0)(\partial\rho/\partial N)$.

The system and the coordinate axes are sketched in figure 1. In the horizontal dimensions (x, y), the medium is of infinite extent and the height is d. Owing to the modified friction term, the system (2.2a)–(2.2d) is of lower order than usual bulk-mixture equations, so only three – rather than four – conditions apply at the upper and the lower boundaries:

$$\left.\begin{aligned} v_z = 0 = \frac{\partial N}{\partial z}+\frac{k_T}{T_0}\frac{\partial T}{\partial z} \quad & \text{at } z = 0, d, \\ T = T_0+\Delta T \quad & \text{at } z = 0, \\ T = T_0 \quad & \text{at } z = d. \end{aligned}\right\} \tag{2.4}$$

It is now not possible to distinguish between free and rigid boundaries for the velocity field, and the only change to free boundary conditions, applied by Brand & Steinberg (1983) and Knobloch (1986), is that of vanishing concentration flux $(\partial N/\partial z)+(k_T/T_0)(\partial T/\partial z)$ at $z = 0,\ d$.

2.1.3. *Heat conduction state and linearized equations*

The condition for stationary heat conduction without convective motion – $\boldsymbol{v} = 0$ and vanishing time derivatives – gives for (2.2*a*)–(2.2*d*) together with (2.3) and (2.4) the solutions for the pure heat conductive state

$$T_c(z) = T_0 + \Delta T(1 - z/d), \tag{2.5a}$$

$$N_c(z) = N_0 + \Delta N(1 - z/d) \quad \text{with } \Delta N = -(k_T/T_0)\,\Delta T, \tag{2.5b}$$

$$\partial p_c/\partial z = -g\rho_0[1 - (\alpha\Delta T - \beta\Delta N)\,(1 - z/d)]. \tag{2.5c}$$

Here ΔN is not given by the boundary condition as it would be in the thermohaline problem (Nield 1967), but through the Soret effect by the applied temperature difference.

Inserting $p(\boldsymbol{r}, t) = p_c(z) + p'(\boldsymbol{r}, t)$, $T(\boldsymbol{r}, t) = T_c(z) + T'(\boldsymbol{r}, t)$ and $N(\boldsymbol{r}, t) = N_c(z) + N'(\boldsymbol{r}, t)$ into (2.2*a*)–(2.2*d*) eventually leads to the equations for the deviations from the heat conduction state. Before writing down, dimensionless units are introduced. Lengths are scaled in units of d and times in units of d^2/κ, so $\boldsymbol{v} = (\kappa/d)\,\boldsymbol{u}$. For the deviations of the temperature and the concentration field the scaling $T' = (\Delta T/R^{\mathrm{por}})\,\theta$ and $N' = -(k_T\,\Delta T/T_0 R^{\mathrm{por}})\,c$ has been chosen. The system is characterized by four dimensionless numbers. The Lewis number L and the separation ratio Ψ are defined as usual:

$$L = D/\kappa, \quad \Psi = \beta k_T/\alpha T_0. \tag{2.6a}$$

It is useful to introduce instead of the bulk Rayleigh number $R^{\mathrm{b}} = (\alpha g d^3/\kappa\nu)\,\Delta T$ a different Rayleigh number R^{por} where the term d^3 is replaced by Kd, and instead of the Prandtl number $P = \nu/\kappa$ an *effective Prandtl number* P_{por} is more natural:

$$R^{\mathrm{por}} = (\alpha g d K/\kappa\nu)\,\Delta T, \quad P_{\mathrm{por}} = \epsilon(d^2/K)P. \tag{2.6b}$$

Together with (2.1) this yields $P_{\mathrm{por}} = P(150(1-\epsilon)^2/\epsilon^2)\,(d/a)^2$. (*For* $P = 10$, $\epsilon = 0.5$ and $d = 10a$ one gets $P_{\mathrm{por}} = 150000$, and in most cases the left-hand side of (2.7*d*) can be neglected.) The linearized equations are then

$$\nabla \cdot \boldsymbol{u} = 0, \tag{2.7a}$$

$$\partial\theta/\partial t = R^{\mathrm{por}} u_z + \nabla^2\theta, \tag{2.7b}$$

$$\partial c/\partial t = R^{\mathrm{por}} u_z + L(\nabla^2 c - \nabla^2\theta), \tag{2.7c}$$

$$\frac{1}{P_{\mathrm{por}}}\frac{\partial(\nabla^2 u_z)}{\partial t} = -\nabla^2 u_z + \frac{\partial^2\theta}{\partial x^2} + \Psi\frac{\partial^2 c}{\partial x^2}, \tag{2.7d}$$

with the boundary conditions

$$u_z = \theta = \frac{\partial c}{\partial z} - \frac{\partial\theta}{\partial z} = 0 \quad \text{at } z = 0, 1. \tag{2.8}$$

To get rid of the pressure term, twice the *curl* has been applied to the Navier–Stokes equation. Because at the convection onset only two-dimensional rolls appear (no y-dependence, see Chandrasekhar 1961; Gershuni & Zhukhovitskii 1976), it is sufficient to consider the equation for u_z. Nonlinear terms in $\boldsymbol{u}$, θ and c have been dropped, because they do not influence the linear convection onset.

2.2. *Narrow cell*

2.2.1. *Hydrodynamic equations and heat conduction state*

A box of infinite length in one horizontal dimension (x) with height d (z-direction) and width b (y-direction) is considered (see figure 2). The governing fluid equations are again (2.2a)–(2.2c) together with the Navier–Stokes equation (Gershuni & Zhukhovitskii 1976):

$$\frac{\partial \boldsymbol{v}}{\partial t}+(\boldsymbol{v}\cdot\boldsymbol{\nabla})\,\boldsymbol{v}=-\frac{1}{\rho_0}\boldsymbol{\nabla}p+\nu\nabla^2\boldsymbol{v}+\frac{\rho}{\rho_0}\boldsymbol{g}. \tag{2.9}$$

Again the Boussinesq approximation, which facilitates the equations, is used here, although its applicability is questionable for really narrow cells leading to large temperature differences. The material parameters are the same as above, except for κ, which is the thermal diffusivity of the fluid. The state equation for ρ is given by (2.3). The boundary conditions are rigid, perfectly heat conducting and impermeable at top and bottom and rigid, adiabatic (temperature isolating) and impermeable on the sidewalls:

$$\left.\begin{aligned} v_z=\frac{\partial v_z}{\partial z}=0=\frac{\partial N}{\partial z}+\frac{k_T}{T_0}\frac{\partial T}{\partial z} \quad & \text{at } z=0,d,\\ T=T_0+\Delta T \quad & \text{at } z=0,\\ T=T_0 \quad & \text{at } z=d, \end{aligned}\right\} \tag{2.10a}$$

$$v_x=v_y=v_z=0=\frac{\partial T}{\partial y}=\frac{\partial N}{\partial y} \quad \text{at } y=0,b. \tag{2.10b}$$

The sidewalls have been chosen to be adiabatic, because only in this limit for $\gamma\to\infty$ do the equations degenerate to those of the porous medium (see below). In the other extreme case of perfectly heat conducting sidewalls the behaviour is completely different (see Frick & Clever (1980) for the simple fluid case).

The heat conduction state is again given by (2.5a)–(2.5c).

2.2.2. *Elimination of the y-dependence and linearized equations*

Inserting again $p(\boldsymbol{r},t)=p_c(z)+p'(\boldsymbol{r},t)$, $T(\boldsymbol{r},t)=T_c(z)+T'(\boldsymbol{r},t)$ and $N(\boldsymbol{r},t)=N_c(z)+N'(\boldsymbol{r},t)$ into (2.2a)–(2.2c) and (2.9) yields for the deviations from the conduction state:

$$\boldsymbol{\nabla}\cdot\boldsymbol{v}=0, \tag{2.11a}$$

$$\frac{\partial T'}{\partial t}+(\boldsymbol{v}\cdot\boldsymbol{\nabla})\,T'=\frac{\Delta T}{d}v_z+\kappa\nabla^2T', \tag{2.11b}$$

$$\frac{\partial N'}{\partial t}+(\boldsymbol{v}\cdot\boldsymbol{\nabla})N'=\frac{\Delta N}{d}v_z+D\left(\nabla^2N'+\frac{k_T}{T_0}\nabla^2T'\right), \tag{2.11c}$$

$$\frac{\partial \boldsymbol{v}}{\partial t}+(\boldsymbol{v}\cdot\boldsymbol{\nabla})\,\boldsymbol{v}=-\frac{1}{\rho_0}\boldsymbol{\nabla}\delta p+\nu\nabla^2\boldsymbol{v}+g(\alpha T'-\beta N')\,\boldsymbol{e}_z. \tag{2.11d}$$

For convection cells which are not too wide, rigid sidewalls lead to a parabolic Poiseuille profile between the lateral boundaries (see e.g. Wooding 1960; Batchelor 1967; Hartline & Lister 1977):†

† For a simple fluid, Frick & Clever (1980) found the differences of the critical values between two- and three-dimensional flow to be a maximum of 1% for $\gamma\approx 0.5$. The differences go to zero very fast for larger and smaller γ.

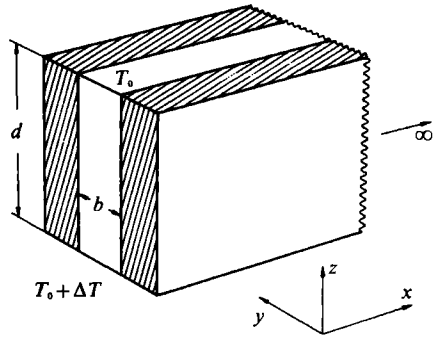

FIGURE 2. The narrow convection channel has the height d, the width b and is of infinite length in the x-direction. All boundaries are rigid for the velocity field and impermeable to mass fluxes. The sidewalls are adiabatic (isolating) for the temperature field, the upper and lower plates are perfectly heat conductors. The temperature at the top plate is T_0 and at the bottom plate $T_0+\Delta T$ with $\Delta T > 0$.

$$v_{x,z}(x,y,z,t) = \bar{v}_{x,z}(x,z,t)f(y), \quad v_y = 0, \Big\} \tag{2.12a}$$

with $$f(y) = (6/b^2)(b-y)y. \Big\}$$

To fulfil the rest of condition (2.10*b*), the y-dependence of T' and N' is also separated out:

$$T'(x,y,z,t) = \bar{T}'(x,z,t)g(y), \quad N'(x,y,z,t) = \bar{N}'(x,z,t)h(y), \Big\} \tag{2.12b}$$

with $$\frac{\partial g}{\partial y} = \frac{\partial h}{\partial y} = 0 \quad \text{at } y = 0, b. \Big\}$$

The y-dependence can be eliminated from (2.11*a*)–(2.11*d*) by inserting the expressions for $\boldsymbol{v}$, T' and N' and averaging the resulting equations over the cell width. The scaling is chosen such that

$$\frac{1}{b}\int_0^b f(y)\,\mathrm{d}y = \frac{1}{b}\int_0^b g(y)\,\mathrm{d}y = \frac{1}{b}\int_0^b h(y)\,\mathrm{d}y = 1.$$

In dimensionless form this yields for the linearized equations valid near the convection onset:

$$\nabla\cdot\boldsymbol{u} = 0, \tag{2.13a}$$

$$\frac{\partial\theta}{\partial t} = R^{\mathrm{HS}}u_z + \nabla^2\theta, \tag{2.13b}$$

$$\frac{\partial c}{\partial t} = R^{\mathrm{HS}}u_z + L(\nabla^2 c - \nabla^2\theta), \tag{2.13c}$$

$$\frac{1}{P_{\mathrm{HS}}}\left(\frac{\partial(\nabla^2 u_z)}{\partial t} - P\nabla^4 u_z\right) = -\nabla^2 u_z + \frac{\partial^2\theta}{\partial x^2} + \Psi\frac{\partial^2 c}{\partial x^2}, \tag{2.13d}$$

with the boundary conditions

$$u_z = \frac{\partial u_z}{\partial z} = \theta = \frac{\partial c}{\partial z} - \frac{\partial\theta}{\partial z} = 0 \quad \text{at } z = 0, 1. \tag{2.14}$$

Again the pressure has been eliminated and the scaling is the same as in §2.1.3 with R^{por} replaced by R^{HS} and P_{por} by P_{HS}:

$$R^{\mathrm{HS}} = \frac{\alpha g d K^{\mathrm{HS}}}{\kappa\nu}\Delta T, \quad P_{\mathrm{HS}} = \frac{d^2}{K^{\mathrm{HS}}}P = 12\gamma^2 P, \tag{2.15a}$$

with $$K^{\mathrm{HS}} = \tfrac{1}{12}b^2. \tag{2.15b}$$

The *effective permeability* K^{HS} replaces K from the porous medium (see Hartline & Lister (1977) for the case of a simple fluid).

2.3. *Analogy between porous medium and narrow cell*

For the limit of infinite effective Prandtl numbers ($K \to 0$ and $\gamma \to \infty$), (2.7d) and (2.13d) both reduce to

$$\nabla^2 u_z = \frac{\partial^2 \theta}{\partial x^2} + \Psi \frac{\partial^2 c}{\partial x^2}. \tag{2.16}$$

(This is the case only for adiabatic sidewalls which facilitate the calculation and lead to the form of (2.13d).)

For the porous medium, this condition is usually fulfilled, whereas in (2.13d) at least the term $(P/P_{\mathrm{HS}})\nabla^4 u_z$ can, in general, not be neglected. For $P = 10$ and $d = 20b$ one has $P_{\mathrm{HS}} = 48000$, which probably is a good approximation to $P_{\mathrm{HS}} \to \infty$, but the term $P/P_{\mathrm{HS}} = 4800$ will still influence the equation. For $d = 2b$ one gets $P_{\mathrm{HS}} = 480$ and (2.16) is not appropriate at all in this case, although (2.13a)–(2.13d) give the correct results.

For the case of a simple fluid there was some confusion in the literature concerning this analogy. The term with $\nabla^4 u_z$ has been neglected from the first by Hartline & Lister (1977), which seems misleading from a theoretical point of view. Although they consider convection experiments in cells with $\gamma = 20$ and $\gamma = 40$, this term still has an influence (see discussion in §4.2 below). It will be shown later, how far the onset values differ for different values of $\gamma = d/b$ and how good the porous medium can be modelled by a narrow cell.

3. Method of solution

Two easily programmable methods have been applied with great success to the bulk binary mixtures: the construction of the exact solutions (Knobloch & Moore 1988; Cross & Kim 1988), which consists of a sum of harmonic functions, and a Runge–Kutta integration scheme (Legros *et al.* 1975; Chock & Li 1975; Schöpf & Zimmermann 1989). It turns out that for the narrow cell the first method is most appropriate and will be used here, while the second one is much slower and converges only over a smaller range of parameters. The Runge–Kutta integration is used to test the results and there are no differences inside the converging regime. For the porous medium it is just the opposite. Therefore both methods are described below.

3.1. *Exact solutions for the narrow cell*

At the convection onset a system of parallel rolls appear with the wavevector $\boldsymbol{k}$ pointing into the x-direction: $\boldsymbol{k} = k\boldsymbol{e}_x$. One solution is

$$\begin{pmatrix} c(x,z,t) \\ \theta(x,z,t) \\ u_z(x,z,t) \end{pmatrix} = \begin{pmatrix} c_0 \\ \theta_0 \\ u_0 \end{pmatrix} \mathrm{e}^{\mathrm{i}kx}\, \mathrm{e}^{qz}\, \mathrm{e}^{\sigma t}. \tag{3.1}$$

Inserting this ansatz into (2.13b)–(2.13d) yields:

$$\begin{pmatrix} \sigma + Lr^2 & -Lr^2 & -R^{\mathrm{HS}} \\ 0 & \sigma + r^2 & -R^{\mathrm{HS}} \\ \Psi k^2 & k^2 & -[(\sigma/P_{\mathrm{HS}})+1]r^2 + (P/P_{\mathrm{HS}})r^4 \end{pmatrix} \begin{pmatrix} c_0 \\ \theta_0 \\ u_0 \end{pmatrix} = 0, \tag{3.2}$$

with $r^2 = k^2 - q^2$. The solvability condition $\det(\ldots) = 0$ leads to a fourth-order characteristic equation for the r_i^2:

$$(\sigma + Lr_i^2)(\sigma + r_i^2)(\sigma + P_{\mathrm{HS}} + Pr_i^2) r_i^2 - R^{\mathrm{HS}} P_{\mathrm{HS}} k^2 (\sigma + Lr_i^2 + \Psi(\sigma + r_i^2 + Lr_i^2)) = 0, \quad (3.3)$$

which for a given k determines the $8 q_i$. At the convection onset the solution is symmetric in z-direction (see Chandrasekhar 1961 for the case of a simple fluid), so for the z-dependent part we have

$$\begin{pmatrix} c(z) \\ \theta(z) \\ u(z) \end{pmatrix} = \sum_{j=1}^{4} \begin{pmatrix} c_0^j \\ \theta_0^j \\ u_0^j \end{pmatrix} A_j \cosh(q_j z), \quad (3.4)$$

with $\theta_0^j = 1$, $c_0^j = 1 + r_j^2/(\sigma + Lr_j^2)$, $u_0^j = (\sigma + r_j^2)/R^{\mathrm{HS}}$ and $q_j^2 = k^2 - r_j^2$.

With the time dependence $\sigma = s + \mathrm{i}\omega$ of (3.1), the solutions are neutrally stable for $s = 0$. For $\omega = 0$ a stationary roll pattern is formed and for $\omega \neq 0$ one has a Hopf bifurcation.

Now the A_j have to be chosen such, that the boundary conditions (2.14) are fulfilled. (The boundaries are shifted from $z = 0, 1$ to $z = \mp\frac{1}{2}$ which is more convenient here.) This leads again to a characteristic equation which for given k determines the corresponding R^{HS} and ω. The convection onset is provided by the lowest R^{HS} on this neutral curve, so at last one ends up with the critical values $R_{\mathrm{c}}^{\mathrm{HS}}$, k_{c} and ω_{c}.

3.2. *Runge–Kutta integration for the porous medium*

The x- and t-dependences of (2.7*b*)–(2.7*d*) are separated by the ansatz

$$\begin{pmatrix} c(x,z,t) \\ \theta(x,z,t) \\ u_z(x,z,t) \end{pmatrix} = \begin{pmatrix} c(z) \\ \theta(z) \\ u(z) \end{pmatrix} \mathrm{e}^{\mathrm{i}kx} \mathrm{e}^{\sigma t} \quad (3.5)$$

leading to

$$\eta'' = \left(\frac{\sigma}{L} + k^2\right)\eta + \frac{\sigma}{L}\theta - \frac{R^{\mathrm{por}}}{L} u, \quad (3.6a)$$

$$\theta'' = (\sigma + k^2)\theta - R^{\mathrm{por}} u, \quad (3.6b)$$

$$u'' = k^2 u - \frac{\Psi k^2 P_{\mathrm{por}}}{\sigma + P_{\mathrm{por}}}\eta - \frac{(1+\Psi) k^2 P_{\mathrm{por}}}{\sigma + P_{\mathrm{por}}}\theta, \quad (3.6c)$$

with $f' := \partial f/\partial z$, $f'' := \partial^2 f/\partial z^2$ and $\eta(z) := c(z) - \theta(z)$. With 6 new functions $y_1 = \theta$, $y_2 = \eta'$, $y_3 = u$, $y_4 = u'$, $y_5 = \theta'$ and $y_6 = \eta$, (3.6*a*)–(3.6*c*) can be rewritten as a 6-dimensional system of first-order differential equations:

$$y_1' = y_5, \quad (3.7a)$$

$$y_2' = \frac{\sigma}{L} y_1 - \frac{R^{\mathrm{por}}}{L} y_3 + \left(\frac{\sigma}{L} + k^2\right) y_6, \quad (3.7b)$$

$$y_3' = y_4, \quad (3.7c)$$

$$y_4' = -\frac{(1+\Psi) k^2 P_{\mathrm{por}}}{\sigma + P_{\mathrm{por}}} y_1 + k^2 y_3 - \frac{\Psi k^2 P_{\mathrm{por}}}{\sigma + P_{\mathrm{por}}} y_6, \quad (3.7d)$$

$$y_5' = (\sigma + k^2) y_1 - R^{\mathrm{por}} y_3, \quad (3.7e)$$

$$y_6' = y_2, \quad (3.7f)$$

with the boundary conditions following from (2.8)

$$y_1 = y_2 = y_3 = 0 \quad \text{at } z = 0, 1. \tag{3.8}$$

With $\boldsymbol{y}$ being the 6-dimensional vector $(y_1(z), y_2(z), \ldots, y_6(z))$, $\boldsymbol{e}_i$ the six 6-dimensional Cartesian unit vectors and $\boldsymbol{\phi}_i$ the 6 linear independent solutions of (3.7*a*)–(3.7*f*) with $\boldsymbol{\phi}_i(0) = \boldsymbol{e}_i$, the general solution is

$$\boldsymbol{y}(z) = \sum_{i=1}^{6} \alpha_i \boldsymbol{\phi}_i(z). \tag{3.9}$$

The boundary conditions (3.8) at $z = 0$ lead to $\alpha_1 = \alpha_2 = \alpha_3 = 0$ so that (3.9) is reduced to

$$\boldsymbol{y}(z) = \sum_{i=4}^{6} \alpha_i \boldsymbol{\phi}_i(z).$$

Runge–Kutta integrations of (3.7*a*)–(3.7*f*) with the boundary conditions $\boldsymbol{e}_4, \boldsymbol{e}_5, \boldsymbol{e}_6$ at $z = 0$ gives $\boldsymbol{\phi}_4(1), \boldsymbol{\phi}_5(1), \boldsymbol{\phi}_6(1)$ and the resulting solution $\boldsymbol{y}(1) = \sum_{i=4}^{6} \alpha_i \boldsymbol{\phi}_i(1)$. The 3 α_i have to be chosen such that the conditions (3.8) are fulfilled at $z = 1$. This is a set of linear equations for the α_i:

$$\begin{pmatrix} \phi_4^1(1) & \phi_5^1(1) & \phi_6^1(1) \\ \phi_4^2(1) & \phi_5^2(1) & \phi_6^2(1) \\ \phi_4^3(1) & \phi_5^3(1) & \phi_6^3(1) \end{pmatrix} \begin{pmatrix} \alpha_4 \\ \alpha_5 \\ \alpha_6 \end{pmatrix} = 0, \tag{3.10}$$

with the solvability condition $\det(\ldots) = 0$. The rest of the procedure is the same as for the exact solutions. With $\sigma = s + \mathrm{i}\omega$, the neutrally stable solution is obtained from the condition $s = 0$. The system (3.7*a–f*) is solved separately for the stationary bifurcation ($\omega = 0$) and the Hopf bifurcation ($\omega \neq 0$). Again for a given k the condition (3.10) yields the corresponding R^{por} and ω and then the critical values $R_{\mathrm{c}}^{\mathrm{por}}$, k_{c} and ω_{c} can be calculated.

4. Results

There are only limited possibilities for testing the numerical calculations. For $\Psi = 0$ the case of a simple fluid has to be recovered, which for the porous medium gives $R_{\mathrm{c}}^{\mathrm{por}} = 4\pi^2$, $k_{\mathrm{c}} = \pi$ and for the narrow cell is reported by Frick & Clever (1980). These values are in full agreement, and for small γ the results for the narrow cell tend to those for bulk mixtures as expected.

With the tools from §3 the critical onset values can now be calculated for different parameter combinations. I have chosen $L = 0.03$, $P = 0.6$, which is appropriate for a ^{3}He–^{4}He mixture consisting typically of 3% ^{3}He (Lee *et al.* 1983; Rehberg & Ahlers 1985; Sullivan & Ahlers 1988) and $L = 0.01$, $P = 10$ for a water–ethanol mixture of typical 0...20% alcohol (Walden *et al.* 1985; Moses & Steinberg 1986; Bensimon *et al.* 1990; Kolodner *et al.* 1990; Schöpf & Rehberg 1992).

4.1. *Overall behaviour for the porous medium*

For $d/a > 5$ one gets for the water–alcohol mixture $P_{\mathrm{por}} > 80000$ and for the ^{3}He–^{4}He mixture $P_{\mathrm{por}} > 5000$. It turns out that for $P_{\mathrm{por}} > 5000$ the $P_{\mathrm{por}} \to \infty$ limit is already attained, so only this limit is considered here.

The results are qualitatively the same as for bulk binary mixtures with realistic boundary conditions (Legros *et al.* 1975; Chock & Li 1975; Knobloch & Moore 1988; Cross & Kim 1988) and this is true also for the narrow cell (see below). Figure 3 shows

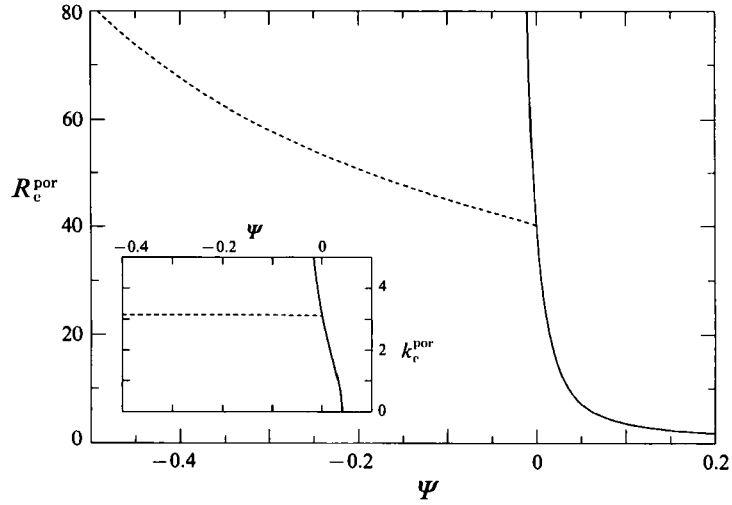

FIGURE 3. Stability diagram for a mixture with $L = 0.03$ in a porous medium in the limit $P_{por} \to \infty$. The solid and dashed lines represent the stationary and the oscillatory bifurcation, respectively. The curves for the critical Rayleigh number R_c^{por} intersect at slightly negative Ψ at the codimension-2 point. The inset shows the dependence of the critical wavenumber k_c^{por} on Ψ, which becomes zero for $\Psi > 0.04$.

the stability diagram for the fluid with $L = 0.03$. Note the scaling for the Rayleigh number which gives $R_c = 4\pi^2$ for $\Psi = 0$. The critical Rayleigh numbers R_c^{stat} (solid line) and R_c^{osc} (dashed line) are equal at the codimension-2 point (CTP) at $\Psi = -2.7 \times 10^{-4}$. Some details of the CTP are discussed in §4.3. For the Hopf bifurcation, the critical wavenumber k_c stays nearly constant over the whole Ψ-regime, while for positive Ψ it rapidly decreases and becomes zero for $\Psi > \Psi_\infty \approx 0.04$ (see inset of figure 3). This feature of zero wavenumber (and therefore infinite wavelength) has been discussed in detail for bulk mixtures by Nield (1967) and Knobloch & Moore (1988). Their method for calculating the value of Ψ_∞ analytically yields, after some tedious algebra,

$$\Psi_\infty = \frac{L}{\frac{40}{51} - L}, \quad R_c = 12\frac{L}{\Psi} \quad \text{for } \Psi > \Psi_\infty. \tag{4.1}$$

A different technique yielding Ψ_∞ is described by Knobloch (1989). The curve for the critical frequency ω_c is not given here, because it is indistinguishable from that shown in figure 4*c* below for $L = 0.01$.

4.2. *Comparison of porous medium with narrow cell*

For the narrow cell, the accessible γ-range is limited for numerical reasons, and the method described above worked only up to $\gamma = 16$. The results are shown in figure 4 for the mixture with $L = 0.01$, $P = 10$ in the porous medium (solid lines), and in the narrow cell for $\gamma = 16$ (dashed lines) and $\gamma = 5$ (dashed-dotted lines).

Figure 4(*a*) shows the critical values for the stationary bifurcation. The approach of the porous medium case for increasing γ can be seen clearly. The differences in R_c between the porous medium and the narrow channel with $\gamma = 16$ are $1.80 \hat{=} 4.5\%$ for $\Psi = 0$ and $0.28 \hat{=} 11\%$ for $\Psi = 0.05$. The situation for the Hopf bifurcation is shown in figure 4(*b*), where the differences in R_c to the porous medium are about 22% for $\gamma = 5$ and 4.5% for $\gamma = 16$. The wavenumbers differ by about 3.5% ($\gamma = 5$) and

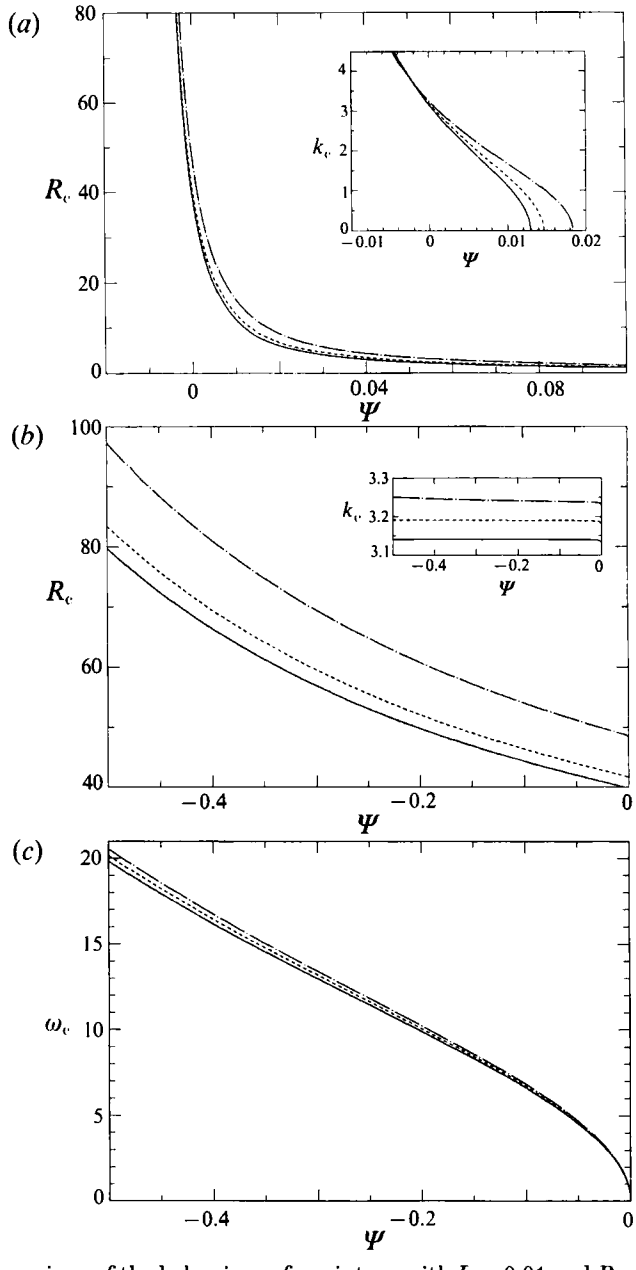

FIGURE 4. Comparison of the behaviour of a mixture with $L = 0.01$ and $P = 10$ in a porous medium (——) and in a narrow cell with $\gamma = 16$ (– – – –) and $\gamma = 5$ (– · – · –). In (*a*) and (*b*) the critical Rayleigh numbers R_c are plotted for the stationary and for the oscillatory bifurcation, respectively. The insets show the corresponding wavenumbers k_c. In (*c*) the critical frequency ω_c for the Hopf bifurcation is shown.

1.6% ($\gamma = 16$). Finally the critical frequency ω_c is shown in figure 4(*c*). Here the differences are about 3.6% for $\gamma = 5$ and 1.6% for $\gamma = 16$. The absolute values are nearly equal for $\Psi \to 0$.

To obtain a better feeling for the tendency to the case of the porous medium, in figure 5 the critical values for the narrow cell are given for $\Psi = -0.4$ as a function

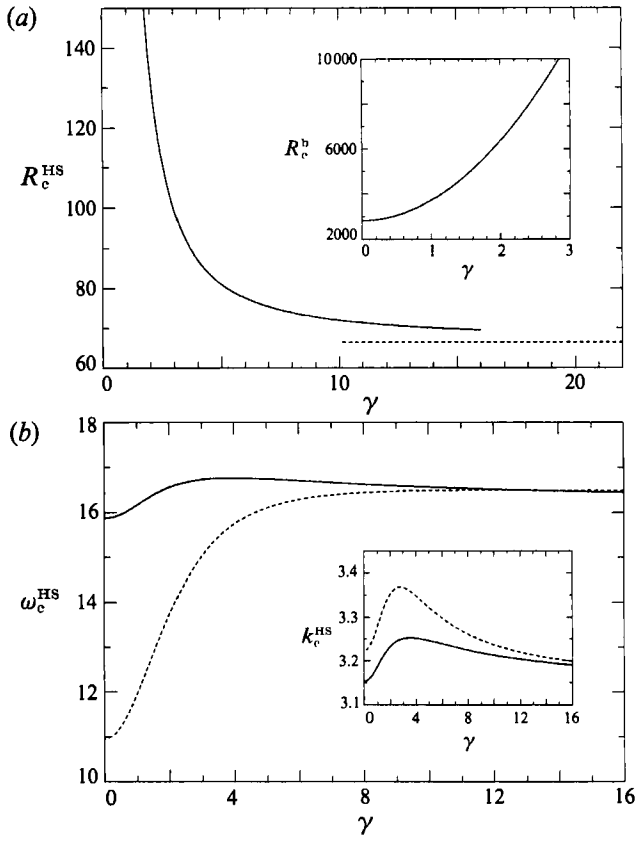

FIGURE 5. Critical values in a narrow cell as a function of γ for $\Psi = -0.4$. The behaviour is analogous for other values of Ψ. In (*a*) the critical Rayleigh number R_c^{HS} for a mixture with $L = 0.01$ and $P = 10$ (——) is plotted which tends very slowly to the value R_c^{por} of the porous medium (– – – –). The inset shows R_c^{HS} rescaled to the value defined for bulk mixtures R_c^b, which tends to the correct value for $\gamma \to 0$. In (*b*) the critical frequency ω_c^{HS} is shown for $L = 0.01$, $P = 10$ (——) and for $L = 0.03$, $P = 0.6$ (– – – –). The dependence is stronger for the lower Prandtl number. The inset shows the respective wavenumbers k_c^{HS} which have a maximum inside the γ-range.

of γ. Figure 5 (*a*) shows R_c^{HS} for $L = 0.01$, $P = 10$ up to the maximal γ-value of 16, the dashed line represents the corresponding $R_c^{por} = 66.42$. The approach to this value is obvious but very slow with increasing γ. To analyse R_c^{HS} for small γ, it has to be rescaled to the value R_c^b defined for bulk mixtures. This is shown in the inset, where for $\gamma = 0$ the correct value $R_c^b = 2819$ is reached. An interesting behaviour is found for the frequency and the wavenumber plotted in figure 5 (*b*) for $L = 0.01$, $P = 10$ (solid lines) and $L = 0.03$, $P = 0.6$ (dashed lines). For the small Prandtl number case ω_c^{HS} depends strongly on γ, while for the other fluid this dependence is weaker, but present. For $\gamma \to 0$ the values are identical to those for bulk mixtures. k_c^{HS} first increases with decreasing γ up to a maximum and then decreases again to the bulk mixture value. This is in contrast to the free, pervious case, where both k_c^{HS} and ω_c^{HS} decrease monotonically from the values for the porous medium to the bulk values. The behaviour for R_c^{HS} and k_c^{HS} is the same for the stationary bifurcation.

The question for which γ a narrow cell is a good approximation to the porous medium depends on the individual problem. Since the characteristics are qualitatively the same for different γ, a cell with $\gamma = 10 \ldots 20$ is sufficient if one is satisfied with an error up to 10%. On the other hand one would need really large γ (up to

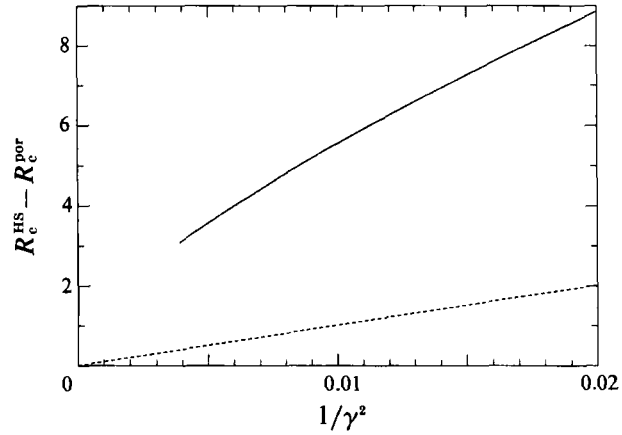

FIGURE 6. The difference between the critical Rayleigh number R_c^{HS} for the narrow cell and the corresponding R_c^{por} for the porous medium is shown as a function of $1/\gamma^2$ for a fluid with $L = 0.01$ and $P = 10$ for $\Psi = -0.4$. For free, pervious boundaries (– – –) this gives a straight line, while this is apparently not the case for rigid, impervious boundaries (——).

50 ... 100) to exactly model a porous medium (see figure 5*a*). For the case of a simple fluid it was speculated by Frick & Clever (1980) that the analogy to the porous medium has already been attained for $\gamma = 20$, which is true only up to 1 or 2 % error. To get the exact results, however, the resolution of their figure 3 is too coarse for this delicate question.

An interesting open question is how for increasing γ the limit of the porous medium is reached. For free, pervious boundaries it can be shown analytically, that $(R_c^{HS} - R_c^{por}) \propto 1/\gamma^2$. In figure 6 this difference is plotted against $1/\gamma^2$ for the free, pervious case (dashed line) and for rigid, impervious boundaries (solid line) for a fluid with $L = 0.01$, $P = 10$ and $\Psi = -0.4$. Whereas the proportionality to $1/\gamma^2$ for the unrealistic boundary conditions is obvious, this seems not to be the case for rigid ones. Although in the interesting regime for large γ the numerics do not work, the solid line points more at another dependency.

4.3. *Codimension-2 point*

For slightly negative Ψ, the critical Rayleigh numbers for the stationary and for the oscillatory bifurcation have the same value R_{CT}. At this CTP the situation is also quite analogous to that in bulk mixtures, which has been discussed in detail by Knobloch & Moore (1988) and Cross & Kim (1988). In our case the CTP is shifted still more against $\Psi = 0$. For $L = 0.03$, $P = 0.6$ one has $\Psi_{CT} = -5.43 \times 10^{-4}$ for the bulk mixture and $\Psi_{CT} = -3.36 \times 10^{-4}$ for $\gamma = 5$, $\Psi_{CT} = -3.02 \times 10^{-4}$ for $\gamma = 16$ and $\Psi_{CT} = -2.7 \times 10^{-4}$ for the porous medium. The wavenumbers at the CTP are different on the two bifurcation branches with k_{CT}^{stat} being slightly larger ($\approx 1.5\%$) than k_{CT}^{osc} and the difference is smaller than in bulk mixtures. As a consequence the critical frequency ω_{CT} is not zero, but has a very small value (≈ 0.04) which is also smaller than in bulk mixtures.

4.4. *Comparison with experiments*

In a recent experiment (Schöpf & Rehberg 1992) a water–ethanol mixture with $L = 0.009$, $P = 10$ and $\Psi = -0.13$ in a cell with $\gamma = 2$ lead to a critical temperature difference of $\Delta T_c \approx 10$K and a critical frequency of $\omega_{c,\,exp} \approx 0.2\ s^{-1}$. This gives for the bulk Rayleigh number $R_{c,\,exp}^{b} \approx 4800$ and for the Rayleigh number according to

(2.15*a*) $R^{HS}_{c,exp} \approx 100$, while the linear stability analysis yield $R^{b}_{c,theo} = 1974$ and $R^{HS}_{c,theo} = 92$. The theoretical values for ω_c for this experiment are $\omega^{b}_{c,theo} = 0.180\ s^{-1}$ and $\omega^{HS}_{c,theo} = 0.186\ s^{-1}$. For the rescaling of the experimental data a mean thermal conductivity $\bar{\kappa}$ has been used to take into account the heat conduction by the sidewalls, because in this experiment the lateral boundaries are not really adiabatic. Thus one cannot expect to get the exact values, but it should be evident, that the critical Rayleigh number for the bulk mixture is completely wrong for the case of the narrow cell, while $R^{HS}_{c,theo}$ is still a good approximation (see footnote on page 268).

The comparison with an experiment of an ^{3}He–^{4}He mixture in a porous medium (Rehberg & Ahlers 1985) is also not simple for other reasons. Here the theory is the correct one, but the properties for this fluid are not known very well. They can be estimated from Brand & Steinberg (1983) yielding, together with the critical values taken from Rehberg & Ahlers (1985), for the bulk Rayleigh number $R^{b}_{c,exp} \approx 230000$, for $R^{por}_{c,exp} \approx 40 \ldots 50$ and for the frequency $\omega_{c,exp} \approx 2$. Obviously one cannot compare this experiment with calculations for the bulk mixture, while a comparison with the values for the porous medium indicate a Ψ of about $-0.02 \ldots -0.05$ which indeed was estimated by Rehberg & Ahlers (1985). For a more precise analysis of this experiment better data for the material parameters are needed.

5. Conclusion

In the present paper the linear stability analysis is given for the convective instability of a binary fluid mixture in a porous medium and in a narrow box subject to an external temperature gradient. In both cases realistic (rigid and impervious) boundary conditions are considered for the first time. It has proven useful to introduce new Rayleigh numbers which take into account the features of the special geometries. The linearized equations for both cases are very similar degenerating to the same set in the limit of infinite effective Prandtl numbers (small K/d^2 and large γ^2) for adiabatic sidewalls in the narrow cell geometry. The parameter values have been chosen to be of direct relevance to experiments in ^{3}He–^{4}He and water–ethanol mixtures.

Whereas the results are analogous to those of bulk mixtures, there are some qualitative differences compared to the case of idealized boundary conditions. Thus the impermeability of the top and bottom plate gives rise to a vanishing wavenumbers on the stationary branch for large enough positive Ψ, in contrast to the idealized case where k_c = constant (depending only on γ in the narrow cell). At the codimension-2 point, where the oscillatory and the stationary instability meet, the wavenumber for both branches are different, leading to a non-vanishing Hopf frequency. In the idealized case the wavenumbers are equal and the frequency is zero. The codimension-2 point itself occurs for Ψ still nearer to zero than in bulk mixtures, so a detailed experimental investigation of the vicinity of this point seems out of reach for liquids.

The analysis of experiments showed that for convection in narrow cells and in a porous medium one cannot compare the data with the results for bulk mixtures, while there is reasonable agreement with the calculations in this paper. For further comparisons more detailed experimental investigations are required.

It is a pleasure to thank I. Rehberg, who gave the motivation to this work, and L. Kramer for fruitful discussions and stimulating criticism.

REFERENCES

Barten, W., Lücke, M., Hort, W. & Kamps, M. 1989 *Phys. Rev. Lett.* **63**, 376.

Batchelor, G. K. 1967 *An Introduction to Fluid Dynamics*. Cambridge University Press.

Bensimon, D., Kolodner, P., Surko, C. M., Williams, H. & Croquette, V. 1990 *J. Fluid Mech.* **217**, 441.

Brand, H. R. & Steinberg, V. 1983 *Physica* **119**A, 327.

Bretherton, C. S. & Spiegel, E. A. 1983 *Phys. Lett.* **96**A, 152.

Chandrasekhar, S. 1961 *Hydrodynamic and Hydromagnetic Stability*. Oxford University Press.

Chock, D. P. & Li, C. 1975 *Phys. Fluids* **18**, 1401.

Cross, M. C. 1988 *Phys. Rev.* A**38**, 3593.

Cross, M. C. & Kim, K. 1988 *Phys. Rev.* A**37**, 3909.

Dullien, F. A. L. 1979 *Porous Media, Fluid Transport and Pore Structure*. Academic Press.

Elder, J. W. 1967 *J. Fluid Mech.* **27**, 29.

Frick, H. & Clever, R. M. 1980 *Z. angew. Math. Phys.* **31**, 502.

Gershuni, G. Z. & Zhukhovitskii, E. M. 1976 *Convective Stability of Incompressible Fluids*. Jerusalem: Keter.

Hartline, B. K. & Lister, C. R. B. 1977 *J. Fluid Mech.* **79**, 379.

Hurle, D. T. J. & Jakeman, E. 1971 *J. Fluid Mech.* **47**, 667.

Irmay, S. 1958 *Trans. Am. Geophys. Union* **39**, 702.

Knobloch, E. 1986 *Phys. Rev.* A**34**, 1538.

Knobloch, E. 1989 *Phys. Rev.* A**40**, 1549.

Knobloch, E. & Moore, D. R. 1988 *Phys. Rev.* A**37**, 860.

Kolodner, P., Glazier, J. A. & Williams, H. 1990 *Phys. Rev. Lett.* **65**, 1579.

Kvernvold, O. & Tyvand, P. A. 1979 *J. Fluid Mech.* **90**, 609.

Lapwood, E. R. 1948 *Proc. Camb. Phil. Soc.* **44**, 508.

Lee, G. W. T., Lucas, P. & Tyler, A. 1983 *J. Fluid Mech.* **135**, 235.

Legros, J. C., Longree, D., Chavepeyer, G. & Platten, J. K. 1975 *Physica* **80**A, 76.

Lhost, O. & Platten, J. K. 1988 *Phys. Rev.* A**38**, 3147.

Lhost, O. & Platten, J. K. 1989 *Phys. Rev.* A**40**, 6415.

Linz, S. J. & Lücke, M. 1987 *Phys. Rev.* A**35**, 3997.

Moses, E. & Steinberg, V. 1986 *Phys. Rev.* A**34**, 693.

Nield, D. A. 1967 *J. Fluid. Mech.* **29**, 545.

Platten, J. K. & Legros, L. C. 1983 *Convection in Liquids*. Springer.

Rehberg, I. & Ahlers, G. 1985 *Phys. Rev. Lett.* **55**, 500.

Schöpf, W. & Kramer, L. 1991 *Phys. Rev. Lett.* **66**, 2316.

Schöpf, W. & Rehberg, I. 1992 *Europhys. Lett.* **17**, 321.

Schöpf, W. & Zimmermann, W. 1989 *Europhys. Lett.* **8**, 41.

Sullivan, T. S. & Ahlers, G. 1988 *Phys. Rev. Lett.* **61**, 78.

Thual, O. & Fauve, S. 1988 *J. Phys. (Paris)* **49**, 1829.

van Saarlos, W. & Hohenberg, P. C. 1990 *Phys. Rev. Lett.* **64**, 749.

Walden, R. W., Kolodner, P., Passner, A. & Surko, C. M. 1985 *Phys. Rev. Lett.* **55**, 496.

Westbrook, D. R. 1969 *Phys. Fluids* **12**, 1547.

Wooding, R. A. 1960 *J. Fluid. Mech.* **7**, 501.